Three Birds with One Stone: Co-Encapsulation of Diclofenac and DL-Menthol for Realizing Enhanced Energy Deposition, Glycolysis Inhibition and Anti-Inflammation in HIFU Surgery

Haitao Wu
Hefei University of Technology
Hu Zhou
Shenzhen Maternity and Child Healthcare Hospital
Wenjie Zhang
Hefei University of Technology
Ping Jin
Shenzhen Maternity and Child Healthcare Hospital
Qianqian Shi
Hefei University of Technology
Zhaohua Miao
Hefei University of Technology
Hua Wang
the First Affiliated Hospital of Anhui Medical University
Zhengbao Zha (zbzha@hfut.edu.cn)
Hefei University of Technology https://orcid.org/0000-0003-3646-4969

Research Article

Keywords: High-intensity focused ultrasound, diclofenac, phase-change, glycolysis inhibition, anti-inflammation

Posted Date: November 29th, 2021

DOI: https://doi.org/10.21203/rs.3.rs-1100333/v1

Abstract

Despite attracting increasing attention in clinic, non-invasive high-intensity focused ultrasound (HIFU) surgery still commonly suffered from tumor recurrence due to the generation of thermo-resistance and adverse therapy-induced inflammation which would promote the secretion of growth signals to trigger tumor recurrence and even metastasis. In this work, inspired by the intrinsic dependence of thermo-resistant heat shock proteins (HSPs) with the adenosine triphosphate (ATP), dual-functionalized diclofenac (DC) with anti-inflammation and glycolysis-inhibition abilities were successfully co-encapsulated with phase-change dl-menthol (DLM) in poly (lactic-co-glycolic acid) nanoparticles (DC/DLM@PLGA NPs) to realize improved HIFU surgery without causing adverse inflammation. Both *in vitro* and *in vivo* studies demonstrated the great potential of DC/DLM@PLGA NPs for serving as an efficient synergistic agent of HIFU surgery, which can not only amplify HIFU ablation efficacy through DLM vaporization-induced energy deposition but also simultaneously sensitize tumor cells to hyperthermia by glycolysis inhibition as well as diminished inflammation. Thus, our study provides an efficient strategy for simultaneously improving the curative efficiency and diminishing the harmful inflammatory responses of clinical HIFU surgery.

Introduction

Benefiting from the efficient sound-to-heat conversion with outstanding temporal-spatial resolution, high-intensity focused ultrasound (HIFU) surgery is an emerging non-invasive treatment modality for localized tumor therapy [1–4]. Although promising and increasingly used in clinic, the ultrasonic energy for HIFU surgery is inevitably attenuated by the different acoustical impedance of human tissues, which could result in insufficient thermal necrosis from a single HIFU treatment and may lead to a risk of residual tumor [5]. In addition, due to the irregular and ambiguous margins of tumor, ordinarily increasing the energy output of HIFU may also bring the adverse normal tissue injury as well as aggravate the pain of patients [6–11]. Moreover, clinical data have confirmed that tumor cells in the HIFU-irradiated central zones always experience thermal coagulative necrosis accompanied by the release of their intracellular reactive oxygen species and other constituents which would trigger a cascade of inflammatory responses [12]. Although the complex relationship between tumor cells and inflammation-related cytokines in the tumor microenvironment is still not fully understood, the post-treatment inflammation have been recognized as adverse effects which were helpful for stimulating tumor metastasis and recurrence [13–19]. Thus, simultaneously improving the curative efficiency and diminishing the harmful inflammatory responses of HIFU surgery is highly pursued.

Among various sensitized strategies for HIFU surgery, the introduction of synergistic agents (SAs) based on biocompatible micro-/nanoparticles especially with some phase-change species has been demonstrated to be an efficient route for enhancing the energy deposition and ultrasonic cavitation in the desired tissues [20–24]. Despite largely improved ablation outcomes can be obtained, the effectiveness of HIFU enhancement is only one-off due to the complete exhaustion of inner core media once the conventional SAs meet HIFU radiation, which could only realize transient cell ablation. Furthermore, the

subsequent adverse harmful inflammatory responses are still in suspense under the utilization of conventional SAs. On the other hand, tumor cells that apart from the HIFU irradiated central zone would commonly activate and up-regulate the expression of intracellular heat shock proteins (HSPs) to establish resistance to heat. As the synthesis of HSPs is highly dependent on adenosine 5’-triphosphate (ATP), blocking the ATP production would be a feasible strategy for weakening the heat-resistance of tumor cells. In comparison to normal tissues, tumor cells are generally characterized with over-expressed glucose transport proteins (Gluts) to uptake much more glucose for rapid growth through energy-inefficient aerobic glycolysis [25–26]. Therefore, it is logical that inhibiting the overexpression of Gluts in tumor cell membranes would reduce the intracellular uptake of glucose and the production of ATP [27–32], which would be beneficial for lowering the expression of HSPs and then sensitizing tumor cells to HIFU surgery.

In this work, diclofenac (DC, a commonly used anti-inflammatory drug in clinic and small molecule inhibitor with high selectivity toward Glut1[33]) and DL-menthol (DLM, a natural phase-change medium) were co-encapsulated in poly(lactic-co-glycolic acid) (PLGA) nanoparticles (DC/DLM@PLGA NPs) *via* the typical oil-in-water emulsion method for simultaneously improving the curative efficiency and diminishing the harmful inflammatory responses of HIFU surgery (Scheme 1a). Once the as-prepared DC/DLM@PLGA NPs accumulated in the tumor region, the thermal effect of HIFU irradiation would induce the phase transition of DLM, which could change the acoustic environment of the tumor site to enhance the ablation effect of HIFU surgery. Subsequently, the released DC would result in down-regulation of Glut1 and consequently inhibit glucose metabolism as well as ATP-dependent HSPs synthesis. Meanwhile, the anti-inflammatory effect of DC reduced the adverse inflammatory responses after HIFU surgery (Scheme 1b).

Result And Discussion

SEM and TEM (Fig. 1a, b) were firstly used to confirm that the as-prepared DC/DLM@PLGA NPs were successfully developed with a relatively uniform spherical morphology. Due to the existence of PVA molecules on their surfaces, the DC/DLM@PLGA NPs were homogeneous dispersed confirmed by the typical Tyndall phenomenon with an average hydrodynamic diameter of around 400 nm (Fig. 1c) and negatively charged with a zeta potential of -27.9 mV (Fig. 1d), respectively. To prove the successful loading of DLM, the aqueous solution of obtained nanoparticles was firstly heated from room temperature to 60°C and then the bubble-generation performance was checked by an inverted fluorescence microscope. As shown in Fig. 1e, the appearance of many bubbles after heating at 60°C was ascribed to the liquid-gas phase transition of DLM, indicating its successful encapsulation in as-prepared NPs which was further confirmed by the result of thermogravimetric analysis showed that the loading content of DLM in DLM@PLGA NPs was approximately 11.8 wt% (Fig. 1f). Benefiting from the characterized UV-vis absorption spectrum of DC, the appearance of an absorption peak at 297 nm demonstrated the successful encapsulation of DC in obtained DC/DLM@PLGA NPs (Fig. 1g), and the loading content of DC was calculated approximately as 10.6% (Additional file 1: Fig. S1). Furthermore, the

as-prepared DC/DLM@PLGA NPs exhibited good dispersity and stability in various media without obvious size change or macroscopic aggregates (Fig. 1h, Additional file 1: Fig. S2).

Next, the *in vitro* synergistic effect of DLM was investigated by using the established experimental platform (Additional file 1: Fig. S3). As shown in Fig. S4, the temperature elevation of PBS solution under HIFU irradiation showed a power-dependent manner and the result demonstrated that the phase transition temperature of DLM could be easily achieved under HIFU irradiation with power input of 25 W for less than 2 min. Without the existence of DLM, the temperature elevation of PLGA aqueous solution (10mg/mL, 600 μL) could achieve 29.2°C under 4 min HIFU irradiation (25 W), while the DLM@PLGA and DC/DLM@PLGA solution increased by 34.5°C and 34.9°C, respectively (Fig. 1i Additional file 1: Fig. S5). This DLM-enhanced temperature elevation could be attributed to the gasified DLM microbubbles which would intercept partial energy of HIFU, reducing the energy loss to the outside and enhancing the acoustic cavitation effect of the ultrasound [34].

Due to the main driven force for DC release was from solid–liquid–gas tri-phase transition of DLM (Fig. 2a), the in vitro DC release behaviors were then first investigated at various temperatures. As shown in Fig. 2b, the amount of released DC was positively correlated with solution temperature. For instance, only 23.6% of DC (these DC molecules were speculated to be encapsulated in PLGA network) was released from the DC/DLM@PLGA NPs within 48 h when the solution temperature was lower than the melting point of DLM. Once the temperature exceeds the melting point of DLM, the amount of released DC increased rapidly. Particularly, due to the strong volatility of DLM and bubbling ability, heating the aqueous solution of DC/DLM@PLGA NPs to 60°C could result in approximately 69.3% of DC release within 12 h. Inspired from the thermo-sensitive DC release profiles, HIFU, as a targeted heat source, was then expected to be appropriate for inducing more controllable drug release as previously reported [35]. With controlled HIFU irradiation for three rounds (5 min each round, power: 25 W; duty cycle: 50%; 3 s on and 3 s off), an enhancement of around 15% of DC release was successfully achieved by the volatilization of DLM caused by HIFU-generated heat and the mechanical effect of HIFU (Fig. 2c) [36], further confirmed by the structure destruction of DC/DLM@PLGA NPs (Fig. 2d). In addition, the bubbling performance of DC/DLM@PLGA NPs under 60°C water bath was further confirmed by naked eyes and monitored by a clinical ultrasound imaging system (Sonix-Touch). Satisfactorily, sustained acoustic signal increments in the in vitro contrast ultrasound image of DC/DLM@PLGA NPs, indicating their good potential for real-time monitoring and programmed DC release (Fig. 2e, Additional file 1: Fig. S6).

The biocompatibility of nanomaterials is a crucial factor that should be firstly considered for potential clinical applications. Following the typical protocol of hemolytic assay, the hemolysis rate of as-prepared DC/DLM@PLGA NPs was determined to be around 4.6% (lower than the threshold value of 5%) even at a dose as high as 800 μg/mL, suggesting the NPs would be relatively safe in the blood circulation (Fig. 3a). Similar satisfactory result was obtained by co-incubation of HUVECs (used here as a normal cell line) with gradient concentrations of NPs. As shown in Fig. 3b, 3c, both standard MTT and CCK-8 assays demonstrated the good cytobiocompatibility of DC/DLM@PLGA NPs as other reported PLGA-based nanoplatform [37, 38]. As the generation of HSPs is highly ATP-dependent, the Glut1 inhibiting property of

DC has been reported to be a potential strategy for weakening the glucose metabolism and thus reducing the ATP level [39]. This inhibitory effect was more obvious on tumor cells with over-expressed Glut1 molecules, which was also consistent with cell-proliferation inhibiting effect of DC confirmed by the typical MTT assay (Additional file 1: Fig. S7) [40]. Therefore, the *in vitro* synergistic effect from HIFU-induced hyperthermia and glucose metabolism inhibition via DC was then investigated by a self-made experimental set-up (Fig. 3d). In comparison to reserved 80% cell viability of DC/DLM@PLGA treated only group, a much more cell killing effect was obtained for DC/DLM@PLGA NPs group under HIFU irradiation (Fig. 3e). In comparison to the DLM@PLGA NPs treated group, the intracellular glucose content in 4T1 tumor cells decreased to 70.9% and 40.4% after treatment with DC/DLM@PLGA NPs for 24 h and 48 h, respectively, which was also lower than the glucose content in HUVECs (Fig. 3f). In addition, the synergistic anti-tumor effect of HIFU surgery and released DC was further visually confirmed by Live/Dead staining. As shown in Fig. 3g, longer HIFU irradiation resulted in more cell death (red fluorescence). In comparison to DLM@PLGA NPs (Additional file 1: Fig. S8), DC/DLM@PLGA NPs could induce more acute cell necrosis under HIFU irradiation which was ascribed to the down-regulated HSPs level in DC-treated 4T1 tumor cells. Thus, benefiting from the over-expressed Glut1 molecules on tumor cells, these obtained results confirmed that DC/DLM@PLGA NPs was relative safe for normal cells and equipped with enhanced cell-killing efficacy on 4T1 tumor cells accompanied with HIFU surgery.

Encouraged by the phase transition capacity of DLM after being heated, DLM-based NPs are supposed to enhance the tumor ablation through DLM vaporization induced energy deposition by both thermal and mechanical effect of HIFU irradiation. After injecting with 100 μL of PBS, PLGA NPs, DLM@PLGA NPs or DC/DLM@PLGA NPs solution, the pork livers were irradiated with HIFU (25 w, 50% duty cycle, 3 s on and 3 s off) for 2 min (Fig. 4a). The area of coagulative necrosis in each liver slice was then measured for characterizing the synergistic ablation effect. The digital photographs (Fig. 4b) and calculated ablation volume of coagulative necrosis areas (Fig. 4c) clearly showed that the ablated areas of pig livers with DLM-encapsulated PLGA NPs (including DLM@PLGA and DC/DLM@PLGA NPs) were significantly larger than those groups without DLM, confirming the enhanced ablation effect of vaporized DLM during localized HIFU surgery.

The *in vivo* tumor inhibition efficacy of HIFU surgery combined with DC/DLM@PLGA NPs was then further evaluated by 4T1 breast tumor-bearing mice. As shown in Fig. 5a, the mice were divided into six groups treated with PBS, DLM/PLGA NPs, DC/DLM@PLGA NPs, PBS + HIFU, DLM/PLGA NPs + HIFU, and DC/DLM@PLGA NPs + HIFU, respectively. The treatment settings was shown in Additional file 1: Fig. S9. Without HIFU irradiation, negligible tumor inhibition effect could be found in the group treated with DLM@PLGA NPs, indicating the good biocompatibility of PLGA-based nanocarriers as previously reported (Additional file 1: Fig. S10) [41, 42]. In consistence with the *in vitro* cell proliferation-inhibiting performance, the tumor growth in the DC/DLM@PLGA NPs treated group was slightly inhibited (Fig. 5b). Satisfactorily, either tumor volume or weight has been observed to be significantly decreased in the presence of HIFU irradiation (Fig. 5c, 5d). As verified in *in vitro* experiments, DLM@PLGA NPs exhibited enhanced tumor inhibition efficacy due to the DLM vaporization induced energy deposition under HIFU irradiation, and the further cooperation with DC yielded the optimal tumor inhibition effect without

obvious recurrence during the two weeks treatment period. Moreover, typical haematoxylin–eosin (H&E) staining of the tumor slices confirmed that cells appeared obviously shrunk and nuclei ruptured after DC/DLM@PLGA + HIFU treatment, which were also observed from the standard TUNEL and Ki-67 staining results (Fig. 5e).

Although hyperthermia has achieved remarkable efficacy in tumor treatment, the acute inflammation induced by the release of intracellular ingredients associated with high temperature also may lead to tumor recurrence and metastasis due to the adverse inflammation. As DC is an anti-inflammatory drug widely used in clinic practice [43, 44], DC-encapsulated DLM@PLGA NPs with the property of inhibition to inflammation after HIFU hyperthermia was desired. After being irradiated by HIFU for 24 h, the serum of mice was taken to detect its levels of inflammatory cytokines. As shown in Fig. 6a-c, HIFU-treated mice with injection of PBS or DLM@PLGA NPs had been detected with significant increases in the level of TNF-α, IL-6, and IL-1β. In dramatic contrast, benefiting from the anti-inflammatory property of DC, the levels of inflammatory cytokines in the DC/DLM@PLGA NPs + HIFU group was significantly decreased. Similarly, immunohistochemical staining of TNF-α, IL-6, and IL-1β also confirmed that DC/DLM@PLGA NPs could effectively alleviate the inflammation caused by HIFU hyperthermia (Fig. 6d). Moreover, the results of pathological examination and blood biochemical analysis of the main organs of mice after the 14 days treatments showed that DC/DLM@PLGA NPs were negligible toxic which could have great potential for clinical applications (Additional file 1: Fig. S11, S12).

Conclusions

In summary, dual-functionalized DC with anti-inflammation and glycolysis-inhibition abilities were successfully co-encapsulated with phase-change medium DLM in PLGA NPs to realize improved HIFU surgery without causing adverse inflammation. The solid-liquid-gas transition of DLM would not only enhance the energy deposition in tumor region during HIFU surgery but also promote the release of encapsulated DC. As a welfare, the released DC molecules inhibited the glucose uptake of tumor cells and subsequently sensitized tumor cells to HIFU surgery through down-regulating the expression of thermo-resistant HSPs. Meanwhile, the anti-inflammatory DC could effectively reduce the occurrence of adverse inflammation caused by HIFU induced coagulative necrosis. Thus, as a proof-of-concept study, our work provides a efficient strategy for simultaneously improving the curative efficiency and diminishing the harmful inflammatory responses of clinical HIFU surgery.

Abbreviations

SEM
Scanning electron microscopy
TEM
transmission electron microscopy
MTT
methyl thiazolyl tetrazolium

CCK-8
Cell Counting Kit-8
PVA
hydrophilic polyvinyl alcohol.

Declarations

Acknowledgments

We acknowledge support of the HaiYing Medical Technology Co., Ltd, Wuxi, China.

Authors' contributions

WH, ZH, and ZZ conceived and designed the experiments, and wrote the manuscript; ZW, SQ and MZ performed partial of the experiments; JP, WH and ZZ coordinated and supervised the work. All authors read and approved the final manuscript.

Funding

This work was supported by the University Synergy Innovation Program of Anhui Province (GXXT-2020-063 and GXXT-2021-066) and the Fundamental Research Funds for the Central Universities (WK9110000176).

Availability of data and materials

All data generated or analyzed during this study are included in this article.

Ethics approval and consent to participate

All animal studies in accordance with the animal protocol approved by Ethics Committees of the Hefei University of Technology (No. HFUT20191015001) and all procedures were in accordance with the Guidelines of the Animal Care and Use Committee of Hefei University of Technology.

Consent for publication

We give our consent for the manuscript to be published in Journal of Nanobiotechnology.

Competing interests

The authors declare that they have no competing interests.

Author details

[1] School of Instrument Science and Opto-Electronics Engineering, School of Food and Biological Engineering, Hefei University of Technology, Hefei, Anhui 230009, P. R. China. [2] Shenzhen Maternity and

Child Healthcare Hospital, Shenzhen, Guangdong 518028, China. [3] Department of Oncology, the First Affiliated Hospital of Anhui Medical University, Inflammation and Immune Mediated Diseases Laboratory of Anhui Province, Anhui 230022, China.

References

[1] Kennedy J. High-intensity focused ultrasound in the treatment of solid tumours. Nat. Rev. Cancer. 2005; 5: 321-327.

[2] Illing R, Kennedy J, Wu F, Haar G, Protheroe A, Friend P, Gleeson F, Cranston D, Phillips R, Middleton M. The safety and feasibility of extracorporeal high-intensity focused ultrasound (HIFU) for the treatment of liver and kidney tumours in a Western population, Brit. J. Cancer. 2005; 93: 890-895.

[3] Wu F. High intensity focused ultrasound: A noninvasive therapy for locally advanced pancreatic cancer. World. J. Gastro. 2014; 20: 16480.

[4] Li C, Zhang W, Fan W, Huang J, Zhang F, Wu P. Noninvasive treatment of malignant bone tumors using high-intensity focused ultrasound. Cancer. 2010 ;116:3934-3942.

[5] Al-Bataineh O, Jenne J, Huber P. Clinical and future applications of high intensity focused ultrasound in cancer. Cancer. Treat .Rev. 2012;38:346-353.

[6] Burke A, Singh R, Carroll D, Wood J, D'Agostino Jr R, Ajayan P, Torti F, Torti S. The resistance of breast cancer stem cells to conventional hyperthermia and their sensitivity to nanoparticle-mediated photothermal therapy. Biomaterials. 2012; 33: 2961-2970.

[7] Calderwood S, Gong J. Trends. Biochem.Sci. 2016; 41: 311-323.

[8] Jego G, Hazoumé A, Seigneuric R, Garrido C. A mitochondrial-metabolism-regulatable carrier-free nanodrug to amplify the sensitivity of photothermal therapy. Cancer. Lett. 2013 ;332:275-285.

[9] N. Tempel, M. Horsman, R. Kanaar, Improving efficacy of hyperthermia in oncology by exploiting biological mechanisms, Inter J Hyperther 2016 (32) 446-454.

[10] Hu J, Cheng Y, Zhang X. Recent advances in nanomaterials for enhanced photothermal therapy of tumors. Nanoscale. 2018; 10:22657-22672.

[11] Wu D, Jin X, Wang X, Ma B, Lou C, Qu H, Zheng J, Zhang B, Yan X, Wang Y, Jing L. Engineering temperature-sensitive plateletsomes as a tailored chemotherapy platform in combination with HIFU ablation for cancer treatment. Theranostics. 2019; 9:3966.

[12] Shin S, Park S, Kim S, Kim M, Kim D. Fluorine MR Imaging Monitoring of Tumor Inflammation after High-Intensity Focused Ultrasound Ablation. Radiology. 2018; 287: 476-484.

[13] Illing R, Kennedy J, Wu F, Haar G, Protheroe A, Friend P, Gleeson F, Cranston D, Phillips R, Middleton M. The safety and feasibility of extracorporeal high-intensity focused ultrasound (HIFU) for the treatment of liver and kidney tumours in a Western population. Brit. J. Cancer. 2005;93: 890-895.

[14] Balkwill F, Charles K, Mantovani A. Smoldering and polarized inflammation in the initiation and promotion of malignant disease. Cancer. cell. 2005; 7: 211-217.

[15] Roxburgh C, McMillan D. The role of the in situ local inflammatory response in predicting recurrence and survival in patients with primary operable colorectal cancer. Cancer Treat. Rev. 2012;38: 451-466.

[16] Hiller J, Perry N, Poulogiannis G, Riedel B, Sloan E. Perioperative events influence cancer recurrence risk after surgery. Nat. Rev. Clin. Oncol. 2018;15:205-218.

[17] Zhou J, Zhao W, Miao Z, Wang J, Ma Y, Wu H, Sun T, Qian H, Zha Z. Folin–Ciocalteu Assay Inspired Polyoxometalate Nanoclusters as a Renal Clearable Agent for Non-Inflammatory Photothermal Cancer Therapy. ACS nano. 2020;14: 2126-2136.

[18] Li Z, Chen Y, Sun Y, Zhang X. Platinum-Doped Prussian Blue Nanozymes for Multiwavelength Bioimaging Guided Photothermal Therapy of Tumor and Anti-Inflammation. ACS nano. 2021; 15: 5189-5200.

[19] Wang S, Zhang C, Chen Z, Ye J, Peng S, Rong L, Liu C Zhang X. A Versatile Carbon Monoxide Nanogenerator for Enhanced Tumor Therapy and Anti-Inflammation. ACS nano. 2019 ;13: 5523-5532.

[20] Luo W, Zhou X, Ren X, Zheng M, Zhang J, He G. Role of enhanced US in evaluating therapeutic response of uterine leiomyoma treated with HIFU. J. Ultras. Med. 2007;26: 419-426.

[21] Xu J, Chen Y, Deng L, Liu J, Cao Y, Li P, Ran H, Zheng Y, Wang Z. Microwave-activated nanodroplet vaporization for highly efficient tumor ablation with real-time monitoring performance. Biomaterials. 2016 ;106:264-275.

[22] Ma M, Xu H, Chen H, Jia X, Zhang K, Wang Q, Zheng S, Wu R, Yao M, Cai X, Li F, Shi J. A drug–perfluorocarbon nanoemulsion with an ultrathin silica coating for the synergistic effect of chemotherapy and ablation by high-intensity focused ultrasound. Adv. Mater. 2014;26: 7378-7385.

[23] K. Zhang, P. Li, H. Chen, X. Bo, X. Li and H. Xu, Continuous Cavitation Designed for Enhancing Radiofrequency Ablation via a Special Radiofrequency Solidoid Vaporization Process, Acs Nano 2016 (10) 2549-2558.

[24] Wang X, Chen H, Zheng Y, Ma M, Chen Y, Zhang K, Zeng D, Shi J. Au-nanoparticle coated mesoporous silica nanocapsule-based multifunctional platform for ultrasound mediated imaging, cytoclasis and tumor ablation. Biomaterials. 2013 ;34: 2057-2068.

[25] Hsu P, Sabatini D. Cancer cell metabolism: Warburg and beyond. Cell. 2008;134: 703-707.

[26] Lincet H, Icard P. How do glycolytic enzymes favour cancer cell proliferation by nonmetabolic functions? Oncogene. 2015 ;34:3751-3759.

[27] Liu Y, Cao Y, Zhang W, Bergmeier S, Qian Y, Akbar H, Colvin R, Ding J, Tong L, Wu S. A small-molecule inhibitor of glucose transporter 1 downregulates glycolysis, induces cell-cycle arrest, and inhibits cancer cell growth in vitro and in vivo. Mol. Cancer. Ther. 2012; 11: 1672-1682.

[28] Hu L, Zhang X, Jiang S, Tao L, Li Q, Zhu L, Yang M, Huo Y, Jiang Y, Tian G. Targeting purinergic receptor P2Y2 prevents the growth of pancreatic ductal adenocarcinoma by inhibiting cancer cell glycolysis. Clin. Cancer. Res. 2019 ;25: 1318-1330.

[29] Zhang T, Wu B, Akakuru O, Yao C, Sun S, Chen L, Ren W, Wu A, Huang P. Hsp90 inhibitor-loaded IR780 micelles for mitochondria-targeted mild-temperature photothermal therapy in xenograft models of human breast cancer. Cancer. Lett. 2021 ;500: 41-50.

[30] Ma Y, Zhou J, Miao Z, Qian H, Zha Z. DL-Menthol Loaded Polypyrrole Nanoparticles as a Controlled Diclofenac Delivery Platform for Sensitizing Cancer Cells to Photothermal Therapy. ACS. Appl. Bio. Mater. 2019 ;2: 848-855.

[31] Jiang A, Liu Y, Ma L, Mao F, Liu L, Zhai X, Zhou J. Biocompatible heat-shock protein inhibitor-delivered flowerlike short-wave infrared nanoprobe for mild temperature-driven highly efficient tumor ablation. ACS. Appl. Mater. Inter. 2019;11:6820-6828.

[32] Gao G, Jiang Y, Guo Y, Jia H, Cheng X, Deng Y, Yu X, Zhu Y, Guo H, Sun W. Enzyme-mediated tumor starvation and phototherapy enhance mild-temperature photothermal therapy. Adv. Funct. Mater. 2020;30: 1909391.

[33] Gottfried E, Lang S, Renner K, Bosserhoff A, Gronwald W, Rehli M, Einhell S, Gedig I, Singer K, Seilbeck A. New aspects of an old drug–diclofenac targets MYC and glucose metabolism in tumor cells. PloS one. 2013;8: e66987.

[34] Coussios C, Farny C, Haar G, Roy R. Role of acoustic cavitation in the delivery and monitoring of cancer treatment by high-intensity focused ultrasound (HIFU). Inter. J. Hyperther. 2007;23: 105-120.

[35] Zhang K, Chen H, Li F, Wang Q, Zheng S, Xu H, Ma M, Jia X, Chen Y, Mou J, Wang X, Shi J. A continuous tri-phase transition effect for HIFU-mediated intravenous drug delivery. Biomaterials. 2014 ;35: 5875-5885.

[36] Zhang K, Li P, He Y, Bo X, Li X, Li D, Chen H, Xu H. Synergistic retention strategy of RGD active targeting and radiofrequency-enhanced permeability for intensified RF & chemotherapy synergistic tumor treatment. Biomaterials. 2016;99: 34-46.

[37] Gao M, Liang C, Song X, Chen Q, Jin Q, Wang C, Liu Z. Erythrocyte-membrane-enveloped perfluorocarbon as nanoscale artificial red blood cells to relieve tumor hypoxia and enhance cancer

radiotherapy. Adv. Mater. 2017;29: 1701429.

[38] Chen Y, Liang Y, Jiang P, Li F, Yu B, Yan F. Lipid/PLGA hybrid microbubbles as a versatile platform for noninvasive image-guided targeted drug delivery. ACS. Appl. Mater. Inter. 2019;11:41842-41852.

[39] Chen W, Luo G, Lei Q, Hong S, Qiu W, Liu L, Cheng S, Zhang X. Overcoming the heat endurance of tumor cells by interfering with the anaerobic glycolysis metabolism for improved photothermal therapy. ACS nano. 2017;11: 1419-1431.

[40] Young C, Lewis A, Rudolph M, Ruehle M, Jackman M, Yun U, Ilkun O, Pereira R, Abel E, Anderson S. Modulation of glucose transporter 1 (GLUT1) expression levels alters mouse mammary tumor cell growth in vitro and in vivo. PloS one. 2011;6: e23205.

[41] Tsirkin S, Goldbart R, Traitel T, Kost J. Tailor-Made Single-Core PLGA Microbubbles as Acoustic Cavitation Enhancers for Therapeutic Applications. ACS. Appl. Mater. Inter. 2021;13: 25748-25758.

[42] Dancy J, Wadajkar A, Connolly N, Galisteo R, Ames H, Peng S, Tran N, Goloubeva O, Woodworth G, Winkles J, Kim A. Decreased nonspecific adhesivity, receptor-targeted therapeutic nanoparticles for primary and metastatic breast cancer. Sci. Adv. 2020;6: eaax3931.

[43] Gan T. Diclofenac: an update on its mechanism of action and safety profile, Curr. Med .Res. Opin. 2010;26:1715-1731.

[44] Roshani A, Falahatkar S, Khosropanah I, Roshan Z, Zarkami T, Palizkar M, Emadi S, Akbarpour M, Khaki N. Assessment of clinical efficacy of intranasal desmopressin spray and diclofenac sodium suppository in treatment of renal colic versus diclofenac sodium alone. Urology. 2010;75:540-542.

Figures

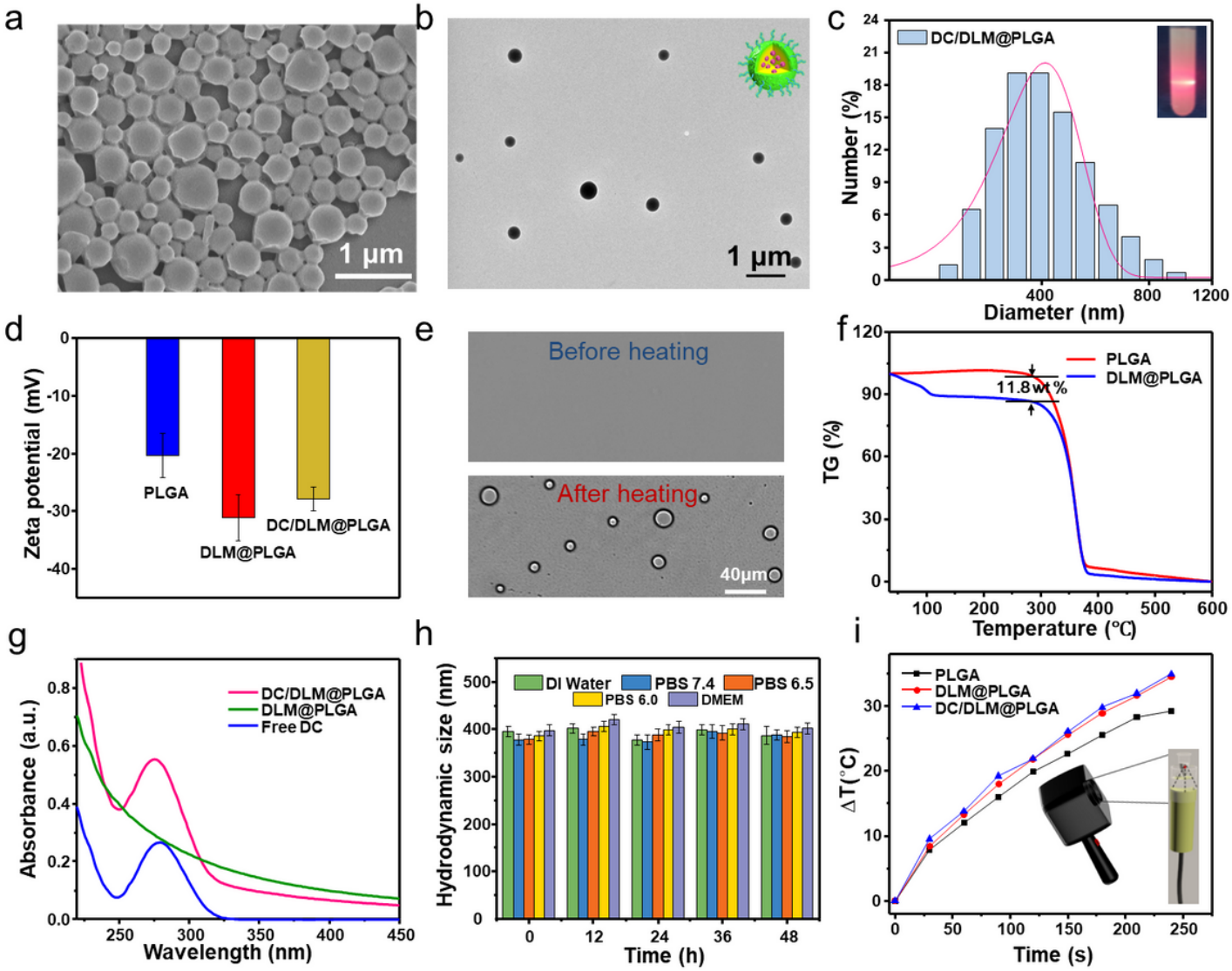

Figure 1

(a) SEM and (b) TEM images of DC/DLM@PLGA NPs. (c) hydrodynamic diameter distribution (inset: Tyndall effect of DC/DLM@PLGA NPs) and (d) zeta potential. (e) Microscopy images of DC/DLM@PLGA NPs under heating for 60 s. (f) TG curve of DC/DLM@PLGA NPs and (g) UV-vis spectra. (h) Stability of DC/DLM@PLGA NPs in various media. (i) Temperature elevation curves of different NPs under HIFU irradiation (power: 25 W; duty cycle: 50%; 3 s on and 3 s off). (Inset: experimental setup for monitoring temperature change by an infrared camera).

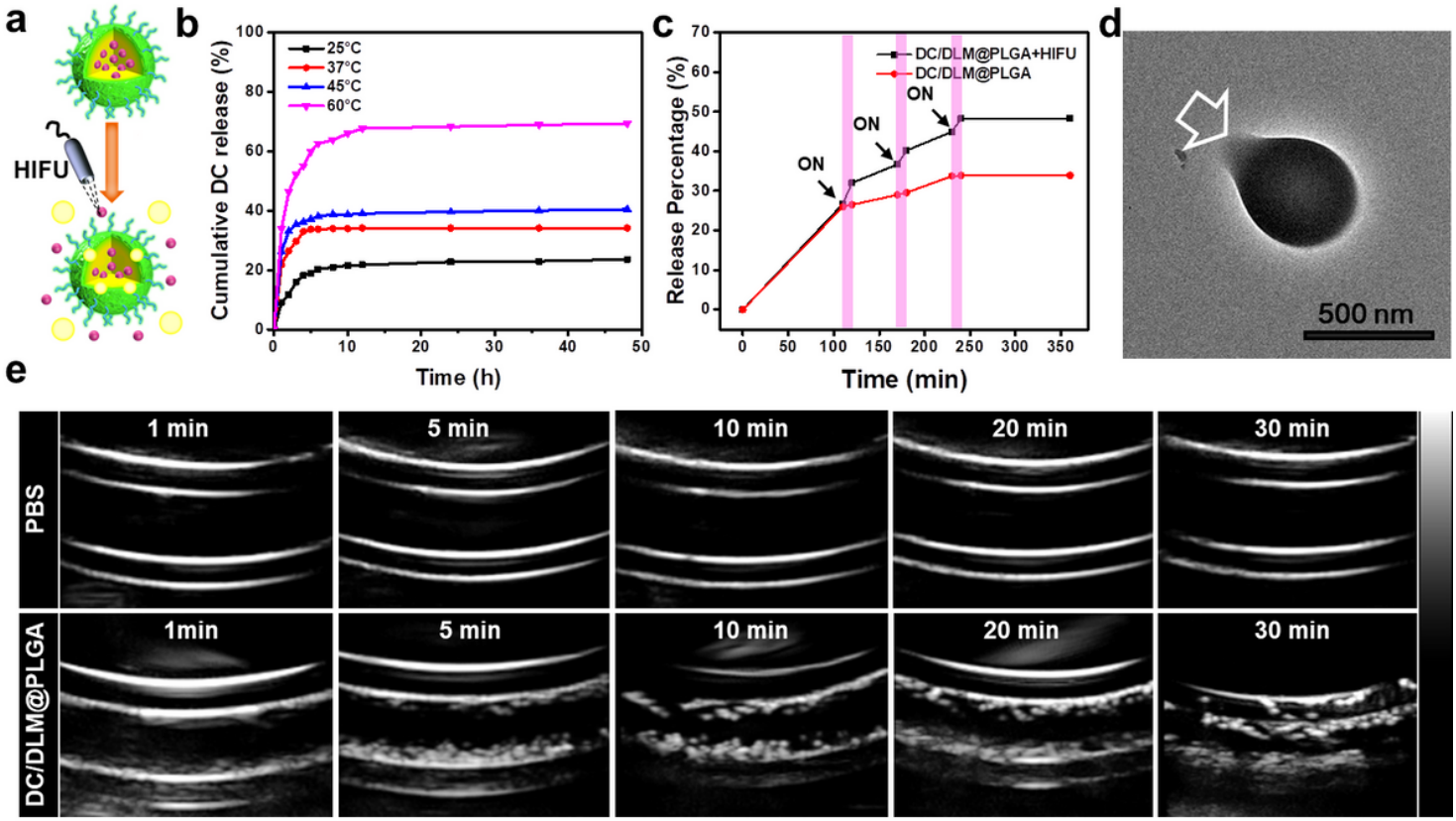

Figure 2

(a) Schematic illustration of DC release from DC/DLM@PLGA NPs under HIFU irradiation. (b) DC release profiles under different temperatures and (c) DC release performances from PLGA nanoparticles triggered by HIFU irradiation. (d) TEM image of typical DC/DLM@PLGA NP after HIFU irradiation. (e) Sustained ultrasonic contrast images of DC/DLM@PLGA NPs (10 mg/mL, 3 mL) in a 60 °C water bath.

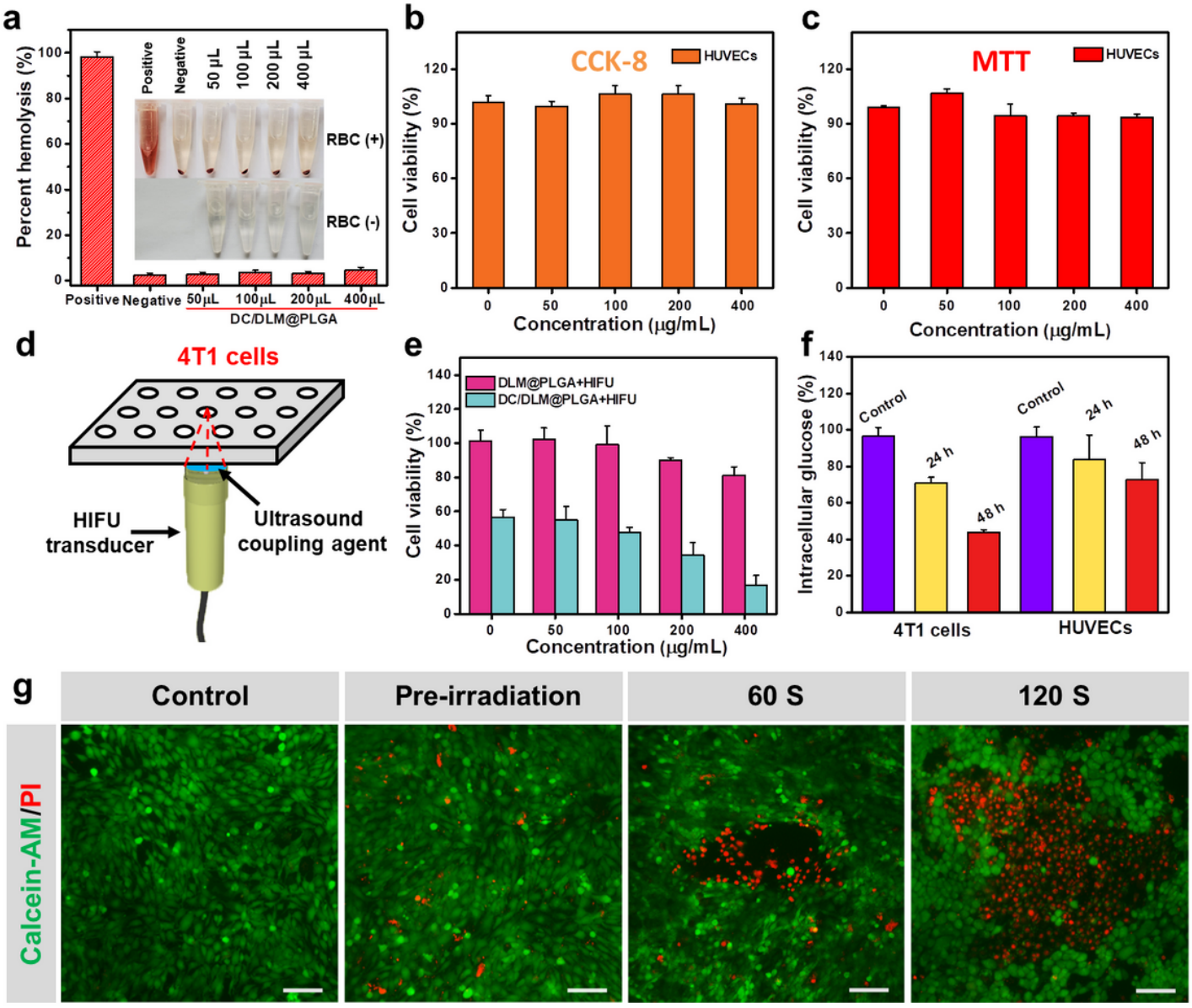

Figure 3

(a) Hemolysis test of DC/DLM@PLGA NPs at different concentrations. (b) MTT and (c) CCK-8 assays. (d) Schematic diagram of experimental setup for 4T1 cells exposed to 50% duty cycle HIFU at 25 W. (e) Cytotoxicity of different DC/DLM@PLGA NPs with gradient concentrations. (f) Intracellular glucose contents of 4T1 cells and HUVECs after co-incubation with DC/DLM@PLGA NPs for 24 h or 48 h. (g) Live/Dead fluorescent staining of 4T1 cells in PBS, DC/DLM@PLGA NPs, and DC/DLM@PLGA NPs + HIFU groups (60 s and 120 s), Scale bar: 100 μm.

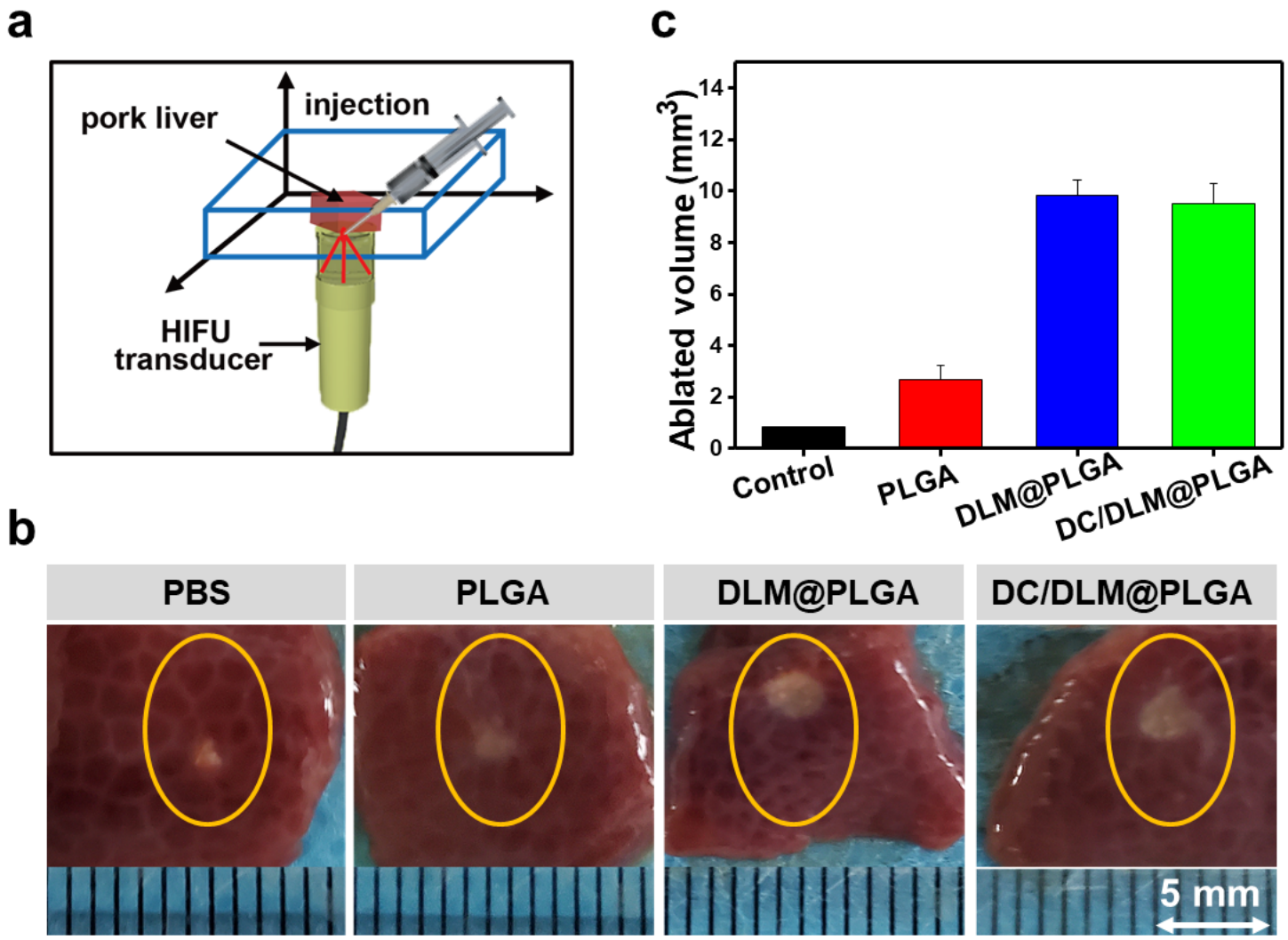

Figure 4

(a) Schematic diagram of experimental setup for in vitro pig liver ablation. (b) Digital photographs of the ablation areas of pig livers after injection of 200 μL solution of PBS, PLGA, DLM@PLGA, or DC/DLM@PLGA NPs and irradiation with HIFU at 25 W and 50% duty cycle for 2 min. (c) Corresponding calculation of the ablation volumes.

Figure 5

(a) Schematic illustration for experimental design. (b) Changes in tumor volumes in different groups of tumor-bearing mice after treatment (*p < 0.05, **p < 0.01). (c) Typical images to tumor tissues. (d) Average tumor weight obtained on the 14th day (*p < 0.05, **p < 0.01); (e) Typical H&E, TUNEL and Ki67 staining of tumor slices. Scale bar: 50 μm.

Figure 6

Detection of serum inflammatory cytokines, including (a) TNF-α, (b) IL-6 and (c) IL-1β in BALB/c mice after different treatments (*p < 0.05, **p < 0.01). (d) Immunohistochemical staining of typical inflammatory cytokines. Scale bar: 50 μm.

Supplementary Files

This is a list of supplementary files associated with this preprint. Click to download.

- 20211121GraphicalabstractHIFU.doc
- 20211121noninflammatoryHIFUSI.docx
- Scheme1.png